Annals of Clinical and Analytical Medicine
Original Research

Is histogram analysis useful in the diagnosis of COVID-19 patients?

COVID-19 patients histogram analysis

Seda Nida Karaküçük[1], Murat Baykara[2], Kezban Tülay Yalçınkaya[3], Selçuk Nazik[4], Fatma Gümüşer[4], Kamil Doğan[1], Adil Doğan[1]
[1] Department of Radiology, Kahramanmaras Sutcu İmam University, School of Medicine, Kahramanmaraş
[2] Department of Radiology, Fırat University, School of Medicine, Elazığ
[3] Department of Molecular Microbiology, Kahramanmaras Sutcu İmam University, School of Medicine, Kahramanmaraş
[4] Department of Infectious Diseases and Clinical Microbiology, Kahramanmaras Sutcu İmam University, School of Medicine, Kahramanmaraş, Turkey

Abstract
Aim: In this study, we aimed to show the contribution of the chest computed tomography (CT)-based histogram analysis method, which will enable us to make quick decisions for patients who are clinically suspected of having COVID-19 infection and whose diagnoses cannot be confirmed by polymerase chain reaction (PCR) tests.
Material and Methods: A total of 84 patients, 40 in the PCR-positive group (age range: 17-90 years) and 44 in the PCR-negative group (age range: 15-75 years), were included in the study. A total of 154 lesions with ground-glass density, 78 in the PCR-positive group and 76 in the PCR-negative group, were detected in these patients' thorax CT scans. The region of interest was placed on the ground-glass opacities from the images and numerical data were obtained by histogram analysis. Numerical data were uploaded to the MATLAB program.
Results: The localizations of ground-glass densities in the CT findings of patients with probable and definite COVID-19 diagnoses were similar; 74.7% of the ground-glass areas in both groups showed peripheral distribution. Lesions were frequently observed in right lungs and lower lobes. In histogram analysis, standard deviation, variance, size %L, size %M, and kurtosis values were higher in the PCR-positive than the PCR-negative group. When receiver operating characteristic curve analysis was performed for standard deviation values, the area under the curve was 0.640, and when the threshold value was selected as 123.4821, the two groups could be differentiated with 62.8% sensitivity and 61.8% specificity.
Discussion: The use of histogram-based tissue analysis, which is a subdivision of artificial intelligence, for clinically highly suspicious patients increases the diagnostic accuracy of CT. Therefore, performing CT analysis with the histogram method will significantly aid healthcare professionals, especially in clinics where rapid decisions are required, such as in emergency services.

Keywords
COVID-19, Histogram Analysis, Chest CT

DOI: 10.4328/ACAM.20744 Received: 2021-06-11 Accepted: 2021-08-20 Published Online: 2022-07-27 Printed: 2022-08-01 Ann Clin Anal Med 2022;13(8):831-835
Corresponding Author: Seda Nida Karaküçük, Department of Radiology, Kahramanmaras Sutcu İmam University School of Medicine, Avşar Mah. West Periphery Blv. No: 251, 46040 Onikişubat, Kahramanmaraş, Turkey.
E-mail: drsedanida@gmail.com P: +90 506 380 36 93
Corresponding Author ORCID ID: https://orcid.org/0000-0002-3789-6571

Introduction

The new coronavirus disease (COVID-19), which was first seen in the city of Wuhan, in China's Hubei province, spread extremely rapidly, causing a global epidemic in a short time. The causative agent of the disease is a single-stranded RNA virus belonging to the family Coronaviridae and it has been named SARS-CoV-2 [1, 2]. Since the beginning of the pandemic, as of May 10, 2021, the World Health Organization states on its official website that more than 190 million cases have been reported worldwide, and more than 4 million of those cases have resulted in death (https://www.who.int/publications/m/item/weekly-epidemiological-update-on-covid-19).

Early diagnosis of coronavirus infection is very important to alleviate and control the spread of this pandemic. Real-time reverse transcription-polymerase chain reaction (RT-PCR) is considered the gold standard for confirming infection. However, its long turn-around time and relatively low sensitivity limit its use [3]. Sometimes, due to insufficient material, RT-PCR tests can be negative even in positive cases. On the other hand, computed tomography (CT) is used as an auxiliary diagnostic tool with 98% sensitivity among COVID-19 patients [4, 5]. In spite of negative RT-PCR tests, positive CT findings can be seen. In addition, CT can be used in the follow-up of COVID-19 infections [6].

Texture analysis is a new field for the quantitative measurement of density changes and concentration of tissues in CT images that cannot be seen with the naked eye. It helps to make image-based decisions about the underlying pathological processes of tissues [7]. Histogram analysis has been used in the evaluation of many lung diseases such as interstitial disease, nodules, and embolisms [8-11]. In histogram-based measurements, the heterogeneity of the tissue can be distinguished by evaluating the gray levels and pixel distributions in the image.

In our study, we aimed to reveal whether there is a difference in CT images between PCR-negative and PCR-positive patients by using the histogram-based texture analysis method in cases of SARS-CoV-2 infection and to show its contribution to diagnosis.

Material and Methods

Ethical approval (Session: 2020/222, Decision No: 02) was obtained from our hospital's ethics committee. The study was conducted between June and September 2020.

Patients

Our study included patients with diagnoses of possible or definite COVID-19 defined according to the guidelines of the Ministry of Health of the Republic of Turkey (https://covid19.saglik.gov.tr/Eklenti/39061/0/covid-19rehberieriskinhastatedavisipdf.pdf). Patients with fever, headache, sore throat, muscle pain, decrease or loss in taste and/or smell, and a history of contact with a COVID-19 patient or with pulmonary involvement compatible with COVID-19 on CT were considered as possible cases.

The RT-PCR test results were negative in two swab samples taken 24 hours apart in probable COVID-19 patients. Patients with positive RT-PCR test results from swab samples taken by combined nasal/oral method were determined as definite COVID-19 cases. Chest CT scans of patients with probable or definite diagnoses were retrospectively re-evaluated by two radiologists (10 and 11 years of experience). Patients with findings of ground-glass density, which is considered a typical finding for COVID-19 on chest CT, were selected. Eighty-four patients and 154 lesions belonging to these patients were included in the study.

Study Design and Image Processing

Lesions with ground-glass density were determined on the chest CT scans of patients with probable and definite COVID-19 diagnoses and were classified according to their locations. Lesions that had contact with the pleura or did not have contact with the pleura but extended parallel to the pleural surface and had less extension to the parenchyma were called subpleural lesions. Lesions adjacent to the pleura that extended

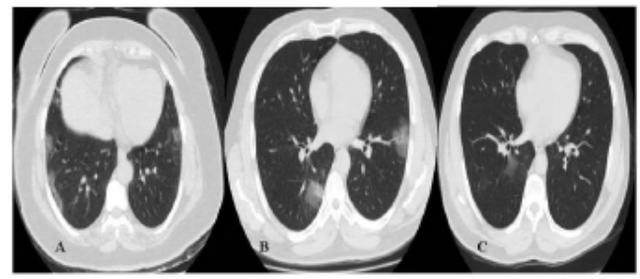

Figure 1. Subpleural (A), Subpleural-parenchymal (B) and parenchymal (C) lesions

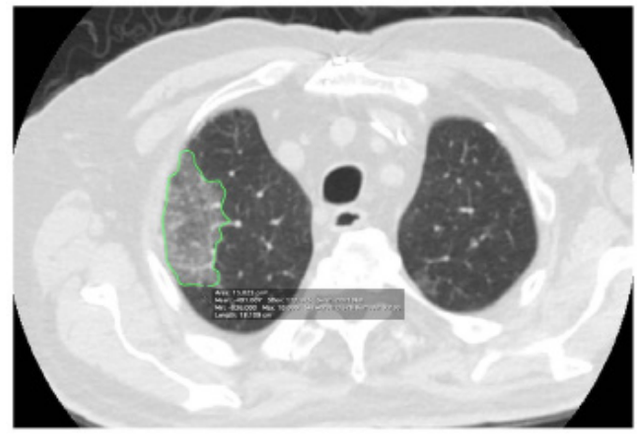

Figure 2. ROI drawing of a subpleural-parenchymal lesion in the upper lobe of the right lung of an RT-PCR positive pateient

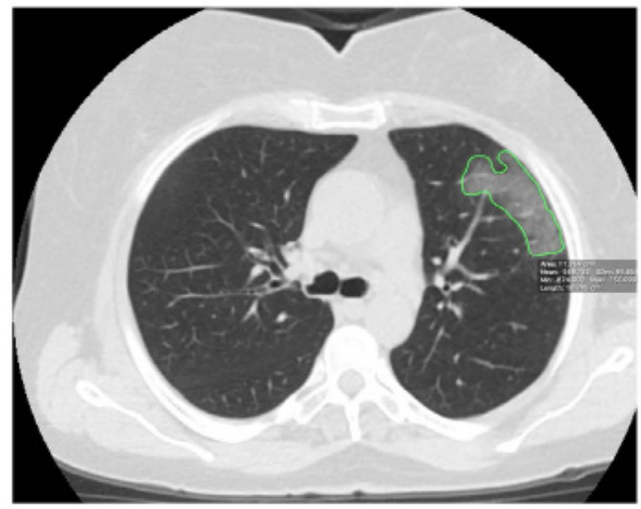

Figure 3. ROI drawing of a subpleural lesion in the upper lobe of the left lung of an RT-PCR negative patient

toward the parenchyma and that had a greater parenchymal extension than the pleural extension were termed subpleural-parenchymal. Lesions located far from the pleura and within the parenchyma were termed parenchymal (Figure 1).

The location of the lesion was also defined as right/left lung and upper/middle/lower lobe. A region of interest (ROI) was placed with a manual drawing surrounding the boundaries of each lesion using the ROI form on a 27-inch iMac computer (Apple Inc., Cupertino, CA, USA) (Figures 2 and 3). Lesions far from vascular structures were preferred in patients with multiple lesions.

CT Examination

Chest CT studies without a contrast agent were performed using a 16-detector-array CT device (Alexion Toshiba Medical Systems, Nasu, Japan) with tube voltage of 120 kVp and tube current of 200 mAs. Slice thickness, reconstruction increment, scan field of view, and matrix size were 3 mm, 0.75 mm, 37 cm, and 512 × 512, respectively. CT images were obtained in the supine position at the full inspiration of the patient.

Statistical Analysis

Histogram analysis from the ROIs was performed using a computer program (Matrix Laboratory, MathWorks Inc., Natick, MA, USA). Mean, standard deviation (SD), minimum, maximum, median, variance, entropy (irregularity), uniformity (inhomogeneity), skewness, and kurtosis values were calculated from the ROIs.

Data were expressed as mean±standard deviation. The chi-square test was used to compare genders and the Mann-Whitney U test was used to compare other parameters of the groups. All statistical analyses were performed with SPSS 25.0 (IBM Corp., Armonk, NY, USA). Values of $p<0.05$ were considered statistically significant.

Results

This study included 40 patients in the PCR-positive group (14 women, 26 men; mean age: 46.4±15.7 years; age range: 17-90 years) and 44 patients in the PCR-negative group (10 women, 34 men; mean age: 43.4±12.6 years; age range: 15-75 years), with a total of 84 patients included. There was no significant difference between the two groups in terms of age or gender ($p>0.05$).

A total of 78 lesions were detected in the CT images of patients with PCR-positive results. Of these lesions, 60.3% were located in the right lung and 39.7% were located in the left lung. A total of 76 lesions were evaluated in the PCR-negative patient group, 60.5% of which were located in the right lung while 39.5% were located in the left lung.

In the PCR-positive group, 52 of 78 lesions were located in the lower, 6 in the middle, and 20 in the upper lobe, while in the PCR-negative group, 40 were located in the lower, 5 in the middle, and 31 in the upper lobe. In both groups, subpleural-parenchymal and subpleural lesions were observed more frequently (45.5% and 29.2%, respectively), while the frequency of parenchymal lesions (25.3%) was lower. While 73.1% of the lesions in the PCR-positive patient group were located in the peripheral region, 74.7% of all lesions were distributed peripherally.

As shown in Table 1, when comparing the PCR-positive group and the PCR-negative group in histogram analysis, there was no significant difference in mean, entropy, skewness, or uniformity values ($p>0.05$), while the standard deviation, variance, size %L, size %M, and kurtosis values were statistically significant different ($p=0.003$, $p=0.003$, $p=0.031$, $p=0.036$, and $p=0.002$, respectively). When receiver operating characteristic (ROC) curve analysis was performed for standard deviation values, the area under the curve (AUC) was 0.640, and when the threshold value was selected as 123.4821, the two groups could be differentiated with 62.8% sensitivity and 61.8% specificity. ROC analysis was also performed for the kurtosis value, yielding an AUC of 0.648, and when the threshold value was selected as 2.8561, the two groups could be differentiated with 61.8% sensitivity and 61.5% specificity.

Table 1. The analysis of histogram parameters of PCR-positive and PCR-negative patients. Statistically significant differences at $p<0.05$.

	PCR-Negative [n=76]		PCR-Positive [n=78]		p*
	Mean	SD	Mean	SD	
Age	43.45	12.62	46.46	15.74	0.342
Mean [HU]	-431.70	170.41	-430.38	173.95	0.905
SD [HU]	117.72	35.13	133.05	33.91	0.003
Minimum [HU]	-761.76	117.36	-768.73	96.86	0.789
Maximum [HU]	-109.93	189.32	-115.00	216.79	0.845
Median [HU]	-420.97	178.63	-420.65	190.16	0.984
Variance	15075.09	9330.40	18838.62	9006.11	0.003
Entropy	7.02	0.38	7.05	0.34	0.593
Size %L	15.96	2.59	16.80	2.45	0.031
Size %M	69.89	5.38	68.24	5.12	0.036
Size %U	14.15	3.61	14.96	3.74	0.084
Kurtosis	4.00	3.77	3.Tem	1.51	0.002
Skewness	-0.16	0.79	-0.16	0.67	0.644
Uniformity	0.31	0.13	0.33	0.13	0.569
Percent01 [HU]	-713.76	129.23	-729.16	114.35	0.499
Percent03 [HU]	-670.49	142.37	-688.56	126.10	0.471
Percent05 [HU]	-642.19	149.42	-661.86	135.17	0.453
Percent10 [HU]	-593.73	160.45	-612.97	151.71	0.453
Percent25 [HU]	-503.97	170.66	-520.12	175.79	0.491
Percent75 [HU]	-351.25	185.49	-334.89	189.97	0.531
Percent90 [HU]	-294.51	184.25	-267.21	181.05	0.334
Percent95 [HU]	-258.50	182.58	-227.65	178.85	0.272
Percent97 [HU]	-233.17	181.37	-204.01	179.92	0.277
Percent99 [HU]	-184.16	179.11	-165.14	187.96	0.504

*: The Mann-Whitney U test was used to compare the groups. SD: Standard deviation.

In both groups, the lesions' locations in the right-left lung or upper-middle-lower lobe did not significantly differ in histogram analysis ($p>0.05$).

Regardless of the location of the lesions, the mean value of the lesions was 377.49±161.03 Hounsfield units (HU) in women and 451.77±171.83 HU in men. When the lesions were examined according to their localization, the mean value was 392.37±164.42 HU for subpleural lesions, 426.17±163.27 HU for subpleural-parenchymal lesions, and 484.34±184.90 HU for parenchymal lesions.

Discussion

The increasing severity of the pandemic and the serious increase

in mortality necessitate the diagnosis of COVID-19 with high accuracy and speed. Although CT findings are typical along with clinical findings, a definite diagnosis of COVID-19 cannot be made from PCR alone as it does not confirm the diagnosis at the time of admission. Therefore, in our study, we hypothesized that we could obtain more data and reduce the contradictions in diagnosis by using a new method, histogram-based tissue analysis, in addition to CT findings in possible and definite COVID-19 cases. Based on our review of the literature, tissue analysis methods have not been used before among COVID-19 patients and our study is the first work in this context.

Chest CT can be used as a screening method to reveal lung findings in potential COVID-19 patients even if the PCR results are negative [12, 13]. In the meta-analysis conducted by Bao et al., examining 13 studies, ground-glass opacities (83.3%) were the most common CT findings of COVID-19. Following this, ground-glass opacities accompanied by consolidation (58.4%), thickening of the adjacent pleura (52.5%), interlobular septal thickening (48.5%), and air bronchograms (46.5%) could be seen. Other CT findings include crazy-paving patterns (14.8%), pleural effusion (5.9%), bronchiectasis (5.4%), pericardial effusion (4.6%), and lymphadenopathy (3.4%) [14]. Although there were different CT findings in our cases, ground-glass density was the most common finding, similar to the literature. Chen et al. evaluated 216 lesions in 33 patients and determined the distribution of peripheral localization for 85% of the lesions [15]. In the study carried out by Song et al., it was found that 86% of the lesions were peripherally located and 90% of them had lower lobe involvement [16]. In our study, similar to the literature, the distribution of lesions was mostly in the lower lobes and peripheral.

Three different basic methods, statistical, model-based, and transform-based, are used in texture analysis [17]. Although statistical methods are the most common among these, texture analysis can also be performed with the histograms of the intensity values of pixels [18]. In other words, histogram-based texture analysis enables quantitative data to be obtained by evaluating the differences in the background's gray-level density. Miles et al. demonstrated how histogram parameters are associated with image analysis [19]. The standard deviation tends to increase with heterogeneous distribution in the tissue. Contrarily, kurtosis tends to decrease with heterogeneity in tissue distribution. There was no significant difference in the number of pixels of the lesions included in both groups in our study. In contrast, the ground-glass areas' gray-level density in the PCR-positive group was observed in a larger area. This led to differences in standard deviation and kurtosis values. On the other hand, this also shows the gray-level changes and the irregularity of the gray-level density in histograms by revealing the relationship of each pixel in terms of entropy and ROI with the neighboring pixels [20]. Another parameter, skewness, shows asymmetry in histograms [21]. The increase in the brightness of pixels shifts the tail of the histogram to the right, causing positive skewness. In our study, the gray-level density of the pixels did not show irregularity or asymmetry in either group. The difference between the size %L and size %M values indicated a difference in the distribution of values in PCR-positive patients.

The limitations of the present study are as follows: As a result of being a single-center study, the number of cases and variety of lesions were low. Also, lung areas with ROIs were not the same in the two groups because the lung area involved was not the same in every individual.

Conclusion

Although chest CT has an important place in diagnosing COVID-19, false-negative PCR results are observed for many patients. The use of histogram-based tissue analysis, which is a subdivision of artificial intelligence, for clinically highly suspicious patients further increases CT's diagnostic accuracy, making chest CT superior to RT-PCR testing. Therefore, performing CT analysis with histograms will significantly aid healthcare professionals, especially in clinics where rapid decisions are required, such as in emergency services.

Scientific Responsibility Statement

The authors declare that they are responsible for the article's scientific content including study design, data collection, analysis and interpretation, writing, some of the main line, or all of the preparation and scientific review of the contents and approval of the final version of the article.

Animal and human rights statement

All procedures performed in this study were in accordance with the ethical standards of the institutional and/or national research committee and with the 1964 Helsinki declaration and its later amendments or comparable ethical standards. No animal or human studies were carried out by the authors for this article.

Funding: *None*

Conflict of interest

None of the authors received any type of financial support that could be considered potential conflict of interest regarding the manuscript or its submission.

References

1. Cascella M, Rajnik M, Cuomo A, et al. Features, evaluation and treatment coronavirus (COVID-19) [e-book]. Treasure Island, FL:StatPearls, 2020

2. Mawaddah A, Gendeh HS, Lum SG, Marina MB. Upper respiratory tract sampling in COVID-19. Malays J Pathol. 2020; 42(1):23-35.

3. Corman VM, Landt O, Kaiser M, et al. Detection of 2019 novel coronavirus (2019-nCoV) by real-time RT-PCR. Euro Surveill. 2020; 25 (3).

4. Fang Y, Zhang H, Xie J, Lin M, Ying L, Pang P, Ji W. Sensitivity of Chest CT for COVID-19: Comparison to RT-PCR. Radiology. 2020 Aug; 296(2):E115-E117.

5. Ai T, Yang Z, Hou H, Zhan C, Chen C, Lv W, Tao Q, Sun Z, Xia L. Correlation of Chest CT and RT-PCR Testing for Coronavirus Disease 2019 (COVID-19) in China: A Report of 1014 Cases. Radiology. 2020; 296(2):e32-e40

6. Guan CS, Wei LG, Xie RM, Lv ZB, Yan S, Zhang ZX, Chen BD. CT findings of COVID-19 in follow-up: comparison between progression and recovery. Diagn Interv Radiol. 2020 Jul; 26(4):301-307.

7. Gillies RJ, Kinahan PE, Hricak H. Radiomics: Images Are More than Pictures, They Are Data. Radiology. 2016 Feb; 278(2):563-77.

8. Koyama H, Ohno Y, Yamazaki Y, Nogami M, Kusaka A, Murase K, et al. Quantitatively assessed CT imaging measures of pulmonary interstitial pneumonia: effects of reconstruction algorithms on histogram parameters. Eur J Radiol. 2016 Feb; 278(2):563-77.

9. Dennie C, Thornhill R, Sethi-Virmani V, Souza CA, Bayanati H, Gupta A, et al. . Role of quantitative computed tomography texture analysis in the differentiation of primary lung cancer and granulomatous nodules. Quant Imaging Med Surg. 2016; 6:6–15.

10. Cohen JG, Reymond E, Medici M, Lederlin M, Lantuejoul S, Laurent F, et al. . CT-texture analysis of subsolid nodules for differentiating invasive from in-situ and minimally invasive lung adenocarcinoma subtypes. Diagn Interv Imaging. 2018; 99:291–9.

11. Sumikawa H, Johkoh T, Yamamoto S, Yanagawa M, Inoue A, Honda O, et al. Computed tomography values calculation and volume histogram analysis for various computed tomographic patterns of diffuse lung diseases. J Comput Assist Tomogr. 2009; 33:731–8.

12. Xie X, Zhong Z, Zhao W, Zheng C, Wang F, Liu J. Chest CT for Typical Coronavirus Disease 2019 (COVID-19) Pneumonia: Relationship to Negative RT-PCR Testing. Radiology. 2020 Aug; 296(2):E41-E45.

13. Raptis CA, Hammer MM, Short RG, Shah A, Bhalla S, Bierhals AJ, Filev PD, Hope MD, Jeudy J, Kligerman SJ, Henry TS. Chest CT and Coronavirus Disease (COVID-19): A Critical Review of the Literature to Date. AJR Am J Roentgenol. 2020 Oct; 215(4):839-842.

14. Bao C, Liu X, Zhang H, Li Y, Liu J. Coronavirus Disease 2019 (COVID-19) CT Findings: A Systematic Review and Meta-analysis. J Am Coll Radiol. 2020 Jun;

17(6):701-709.
15. Chen ZH, Li YJ, Wang XJ, Ye YF, Wu BL, Zhang Y, Xuan WL, Bao JF, Deng XY. Chest CT of COVID-19 in patients with a negative first RT-PCR test: Comparison with patients with a positive first RT-PCR test. Medicine(Baltimore). 2020 Jun 26; 99(26):e20837.
16. Song F, Shi N, Shan F, Zhang Z, Shen J, Lu H, Ling Y, Jiang Y, Shi Y. Emerging 2019 Novel Coronavirus (2019-nCoV) Pneumonia. Radiology. 2020 Apr; 295(1):210-217. Epub 2020 Feb 6. Erratum in: Radiology. 2020 Dec; 297(3):E346.
17. Davnall F, Yip CS, Ljungqvist G, et al. Assessment of tumor heterogeneity: an emerging imaging tool for clinical practice? Insights Imaging 2012; 3(6):573–589.
18. Varghese BA, Cen SY, Hwang DH, et al. Textureanalysis of imaging: what radiologists need to know. AJR Am J Roentgenol 2019; 212(3):520–8.
19. Miles KA, Ganeshan B, Hayball MP. CT texture analysis using the filtration-histogram method: what do the measurements mean? Cancer Imaging. 2013 Sep 23; 13(3):400–6
20. Hodgdon T, McInnes MDF, Schieda N, Flood TA, Lamb L, Thornhill RE. Can Quantitative CT Texture Analysis be Used to Differentiate Fat-poor Renal Angiomyolipoma from Renal Cell Carcinoma on Unenhanced CT Images? Radiology. 2015 Sep; 276(3):787–96.
21. Zhang G-M-Y, Shi B, Xue H-D, Ganeshan B, Sun H, Jin Z-Y. Can quantitative CT texture analysis be used to differentiate subtypes of renal cell carcinoma? Clin Radiol. 2019 Apr; 74(4):287-94.

How to cite this article:
Seda Nida Karaküçük, Murat Baykara, Kezban Tülay Yalçınkaya, Selçuk Nazik, Fatma Gümüşer, Kamil Doğan, Adil Doğan. *Is histogram analysis useful in the diagnosis of COVID-19 patients?. Ann Clin Anal Med 2022;13(8):831-835*